arXiv:1601.05985v1 [cond-mat.soft] 22 Jan 2016

Computing optimal interfacial structure of modulated phases

Jie Xu[1], Chu Wang[2], An-Chang Shi[3] and Pingwen Zhang[1*]

[1]LMAM & School of Mathematical Sciences, Peking University, Beijing 100871, China
[2]Program in Applied and Computational Mathematics, Princeton University,
Princeton, New Jersey 08544, USA
[3]Department of Physics and Astronomy, McMaster University,
Hamilton, Ontario L8S4M1, Canada
Email: rxj_2004@126.com, chuw@math.princeton.edu, shi@mcmaster.ca, pzhang@pku.edu.cn

January 25, 2016

Abstract

We propose a general framework of computing interfacial structures between two modulated phases. Specifically we propose to use a computational box consisting of two half spaces, each occupied by a modulated phase with given position and orientation. The boundary conditions and basis functions are chosen to be commensurate with the bulk structures. It is observed that the ordered nature of modulated structures stabilizes the interface, which enables us to obtain optimal interfacial structures by searching local minima of the free energy landscape. The framework is applied to the Landau-Brazovskii model to investigate interfaces between modulated phases with different relative positions and orientations. Several types of novel complex interfacial structures are obtained from the calculations.

Keywords: Interface; Modulated phase; Metastable state; Compatibility; Landau-Brazovskii model.

1 Introduction

Interfaces are transition regions connecting two different materials, two different phases of the same material, or two grains of the same phase with different orientations (grain boundaries). Interfacial regions are where the symmetries and patterns of the ordered structures are interrupted. Therefore, the structure of interfaces greatly affects the mechanical, thermal and electrical properties of a material. Interfaces are frequently encountered as planar defects in phase transitions. In particular, the strength and conductivity of a material depend strongly on the distribution and morphology of grain boundaries. In first-order phase transitions, the interfacial properties play an important role in the nucleation-growth process.

Theoretical discussions of interfaces usually start from the coexistence of two homogeneous phases, namely the order parameters are spatially uniform in equilibrium. If the contribution of inhomogeneity is included in the free energy, the interfacial structure becomes an intrinsic

*Corresponding author

property of the energy functional. A simple but widely-used energy functional of this model system is proposed by Cahn and Hilliard [1]. Since interfaces are non-equilibrium structures with long relaxation time, two different points of view can be held. One regards the interface as a metastable state and its morphology is considered as a local minimizer of the free energy under certain constraints. The minimization approach is able to reach full relaxation and resolves the interfacial structure. This approach has been applied to two-component fluid interfaces to study the thickness and shape in various circumanstances [1, 2, 3, 4, 5], as well as isotropic-nematic interfaces in liquid crystals [3, 6, 7]. An alternative approach is to treat the interface as a transient state and focuses on its dynamics, based on the free energy, in some complex processes (see [8, 9] for two examples built on the Cahn-Hilliard energy). The dynamical approach enables the study of the dynamical evolution of interfaces.

Interfaces between modulated phases have unique features. Because of spatial modulation, the interfacial profile depends on the relative position and orientation of the phases. Also interfaces may exist between two grains of the same phase, i.e. grain boundaries. These features make it extremely interesting to study the mechanism of how two modulated structures are connected, which is very helpful to understanding the origin of epitaxial relationship and the anistropic nucleation. Therefore, it is important to investigate the morphology of a single interface using the minimization approach. In previous studies, the minimization approach has been used successfully in the tilted grain boundaries of the lamellar phase [10, 11, 12, 13] and the bcc phase [14], and twist grain boundaries of several cubic phases [15]. Some works use dynamical apporach [16, 17, 18], but it usually generates several interfaces because there is limitation in choosing boundary conditions, which we will explain later in detail. From the view of computation, dynamical approach is more time-consuming, while in the minimization approach fast optimization algorithms can be used. In what follows, our discussion is limited to the minimization approach.

To convert a non-equilibrium interface into a metastable state, we need some anchoring conditions. Let us explain the anchoring conditions using a planar liquid-vapor interface as an example, where the density ϕ can be viewed as varying only in the x-direction. Suppose that the density of the liquid is ϕ_1, and that of the vapor is ϕ_2. The density far away from the interface shall be identical to the bulk values,

$$\phi(-\infty) = \phi_1, \ \phi(+\infty) = \phi_2. \tag{1}$$

Note that these conditions do not determine the location of the interface. If we want to fix it, say, at $x = 0$, an extra constraint is needed. A possible constraint is to choose an interval $[-L, L]$ and fix the total number of molecules in it,

$$\int_{-L}^{L} \mathrm{d}x \ \phi(x) = N. \tag{2}$$

The constraint can easily be extended to the study of interfaces of other shapes on substrate or with external forces [4, 5]. The conditions (1) and (2) are both physical, and are sufficient to pose the interfacial profile as a minimization problem.

For interfaces between two modulated phases, the anchoring conditions are not straightforward to specify. We need to consider the relation between the conditions and the bulk profiles. Since the anchoring conditions actually specify the function space in which the minimization problem is solved, we may evaluate how good the conditions are by comparing the

function space with the bulk profiles. If the bulk profiles are included in the function space, we say that the anchoring conditions are compatible. The condition (1) is compatible, and it becomes incompatible if we set $\phi(+\infty)$ to a value other than ϕ_2. We believe that compatibility would be more significant for modulated phases, because we need to anchor the phases with given relative position and orientation. Besides the compatibility, the anchoring shall include as few artificial restrictions as possible to enable the free relaxation of the interface.

In previous works, however, the compatibility and the reduction of artificial effects are usually not considered simultaneously. As a simple extension of the disordered interfaces, some works construct the interface profile by a mixing ansatz, which is the direct weighted combination of two bulk phase profiles:

$$\phi(x,y,z) = (1-\alpha(x))\phi_1(x,y,z) + \alpha(x)\phi_2(x,y,z) \tag{3}$$

where ϕ_k are profiles of two bulk phases, and $\alpha(x)$ is a smooth monotone function satisfying $\alpha(-\infty) = 0,\ \alpha(+\infty) = 1$. This method proves to be convenient and effective as shown in the literatures [3, 19, 20]. But this artificial approach may exclude the possibility of complex interfacial structures as we will present later in this paper. Another convenient method is to fill a large cell with modulated structures and let the interface relax itself (see, for example, [16]). However, besides the computational challenges, the boundary conditions commonly used and the bulk structures are incompatible. Although large-cell computations have brought some beautiful results in [10], where considerable efforts are made to fit the bulk structures with the boundary, the incompatibility may easily generate many interfaces together, like Fig. 5.20 in [21]. On the other hand, it may alter the position and orientation of the bulk structures from the desired values, or even destroy the bulk structures (see the examples in [17]).

There have been attempts to balance between anchoring bulk structures and reducing the artificial effects. In the study of kink [11] and T-junctions [13] in lamellar grain boundaries, a set of basis functions are carefully chosen to retain symmetry properties. However, the basis functions are only partially compatible with the lamellar structure, and they cannot be easily extended to other structures. Therefore, we aim to propose compatible anchoring conditions with universal applicability and no artificial effects.

When investigating an interface between different phases, a mechanism is required to prevent it from moving gradually towards the phase with higher energy density. We may choose parameters to equalize the energy densities, but it is difficult to realize in computation. Intuitively, we need to propose an analog of the constraint (2). However, we observe in the computation that constraints of such kind are not necessary if the bulk phases are modulated. The interface will be pinned at a locally optimized position as long as the energy densities of the two phases do not differ too much. Thus we may let the interface freely relax itself during the computation instead of intervening in the process.

In this work, we propose a general framework for the computation of interfacial structures between modulated phases. We consider two phases or grains, large in size, connected via an interfacial region. We choose basis functions compatible with the bulk structures in two directions parallel to the contact plane, and use a compatible boundary anchoring analogous to (1) in the direction vertical to the plane. The computational setting is applicable to any modulated phases, and is well-posed as a minimization problem for phases with energy difference. By this setting, we can take the advantage of full relaxation of the system and fast optimization methods. We will apply this framework to the Landau-Brazovskii model

to illustrate the above features. Several lamellar-gyroid and cylindral-gyroid interfaces with different relative positions and orientations are examined, and some complex structures are acquired. The rest of the paper is organized as follows. In Sec. 2, the computational framework is described, and its well-posedness is illustrated. Some interfacial structures in the Landau-Brazovskii model are presented in Sec. 3. Finally we summarize the paper in Sec. 4. Some details of numerical method are given in Appendix.

2 Computational framework

2.1 Compatible anchoring conditions

When two ordered structures contact each other, their spatial and orientational relations are essential variables. Let us place the two phases in two half-spaces separated by the plane $x = 0$. Denote the two phases by α and β respectively. Both phases can be rotated and displaced, represented by the orthogonal rotation matrices $\mathcal{R}_\alpha$, $\mathcal{R}_\beta$, and the displacement vectors $\boldsymbol{d}_\alpha$, $\boldsymbol{d}_\beta$. Each of these four quantities has three degrees of freedom. Note that the relation of two phases remains unchanged if they are rotated together round the x-axis or shifted together in the y-z plane, so there are nine independent degrees of freedom in total.

Assume that the density profile, or order parameter, of a phase can be expressed by a scalar function ϕ. More specifically, we assume that ϕ is periodic, which can be written as

$$\phi(\boldsymbol{r}) = \sum_{\boldsymbol{k}\in\mathbb{Z}^3} \phi_{\boldsymbol{k}} \exp\left(i \sum_{j=1}^{3} k_j \boldsymbol{b}_j \cdot \boldsymbol{r} \right). \tag{4}$$

If the phase is rotated by $\mathcal{R}$, then shifted by $\boldsymbol{d}$, the profile becomes

$$\phi(\boldsymbol{r}; \mathcal{R}, \boldsymbol{d}) = \phi(\mathcal{R}^T(\boldsymbol{r} - \boldsymbol{d})) = \sum_{\boldsymbol{k}\in\mathbb{Z}^3} \phi_{\boldsymbol{k}} \lambda_{\boldsymbol{k}} \exp\left(i \sum_{j=1}^{3} k_j (\mathcal{R}\boldsymbol{b}_j) \cdot \boldsymbol{r} \right), \tag{5}$$

where $\lambda_{\boldsymbol{k}} = \exp(-i \sum_{j=1}^{3} k_j \boldsymbol{d}^T \mathcal{R} \boldsymbol{b}_j)$.

As mentioned above, we aim to propose anchoring conditions with compatibility. First we check the y- and z-directions. Consider the projection of profile ϕ_α and ϕ_β onto the plane $x = x_0$. Denote $\boldsymbol{r}' = (y, z)$. Then we have

$$\phi_\alpha(x_0, \boldsymbol{r}'; \mathcal{R}_\alpha, \boldsymbol{d}_\alpha) = \sum_{\boldsymbol{k}\in\mathbb{Z}^3} \phi_{\alpha\boldsymbol{k}} \tilde{\lambda}_{\alpha\boldsymbol{k}} \exp\left(i \sum_{j=1}^{3} k_j \boldsymbol{b}'_{\alpha j}(\mathcal{R}_\alpha) \cdot \boldsymbol{r}' \right),$$

where $\boldsymbol{b}'_{\alpha j}(\mathcal{R}_\alpha)$ denotes the y and z components of $\mathcal{R}_\alpha \boldsymbol{b}_{\alpha j}$, and $\tilde{\lambda}_{\alpha\boldsymbol{k}} = \lambda_{\alpha\boldsymbol{k}} \exp\left(i x_0 \sum_{j=1}^{3} k_j (\mathcal{R}_\alpha \boldsymbol{b}'_{\alpha j})_1 \right)$. It becomes a quasiperiodic function in the plane. And for ϕ_β, we have

$$\phi_\beta(x_0, \boldsymbol{r}'; \mathcal{R}_\beta, \boldsymbol{d}_\beta) = \sum_{\boldsymbol{k}\in\mathbb{Z}^3} \phi_{\beta\boldsymbol{k}} \tilde{\lambda}_{\beta\boldsymbol{k}} \exp\left(i \sum_{j=1}^{3} k_j \boldsymbol{b}'_{\beta j}(\mathcal{R}_\beta) \cdot \boldsymbol{r}' \right).$$

Then a natural choice will be the set of quasiperiodic function

$$\mathcal{F} = \left\{ f(\boldsymbol{r}') : f(\boldsymbol{r}') = \sum_{\boldsymbol{k},\boldsymbol{l}\in\mathbb{Z}^3} f_{\boldsymbol{k}} \exp\left(i \sum_{j=1}^{3} \left(k_j \boldsymbol{b}'_{\alpha j}(\mathcal{R}_\alpha) + l_j \boldsymbol{b}'_{\beta j}(\mathcal{R}_\beta) \right) \cdot \boldsymbol{r}' \right) \right\}. \tag{6}$$

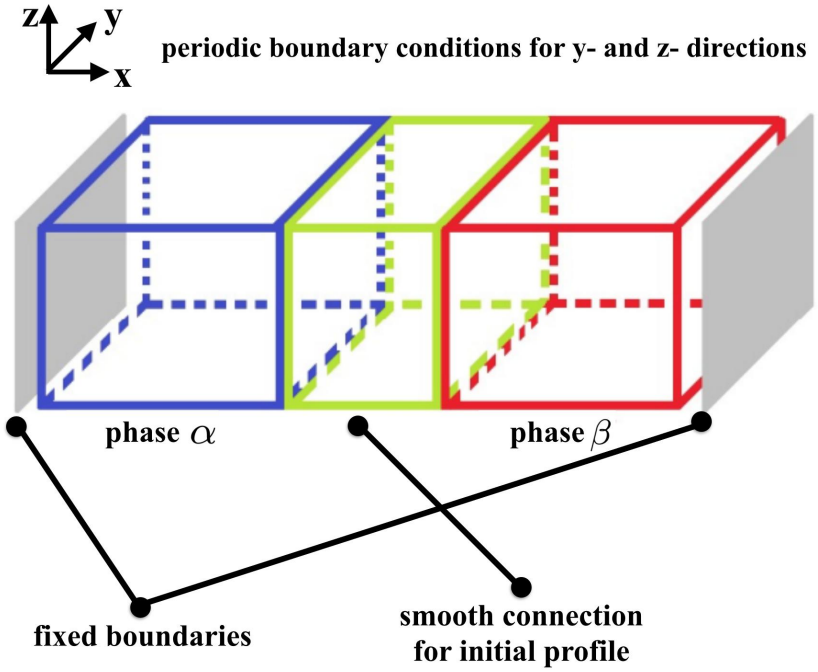

Fig. 1: Schematic of the setting of interface problem.

In general, a quasiperiodic function is a projection of a higher-dimensional periodic function onto a lower-dimensional linear subspace. Actually, this choice is also valid if ϕ itself is quasiperiodic, namely to substitute the sum over $1 \le j \le 3$ with $1 \le j \le m$. In special cases where $k_j \boldsymbol{b}'_{\alpha j}(\mathcal{R}_\alpha) + l_j \boldsymbol{b}'_{\beta j}(\mathcal{R}_\beta)$ lie on a 2D lattice, $\mathcal{F}$ is reduced to a set of periodic functions, indicating that two phases, with their relative position and orientation determined, have common period in the y-z plane. The current work will focus on these special cases. Despite we do not consider the general quasiperiodic cases currently, interfaces of this type have been observed (see Fig. 24 of [22]).

In the x-direction, we select a length L and set ϕ outside $[-L, L]$ equal to the bulk value. Here L is large enough to contain the transition region. Such setting will induce some anchoring conditions at $x = \pm L$ dependent on the energy functional. If a Laudau-type energy functional is used, these conditions can usually be determined by smoothness requirements of the density profile ϕ. For example, if ϕ is C^k, then $\phi, \ldots, \nabla^k \phi$ shall be fixed to bulk values at $x = \pm L$. It should be noted that in some other models boundary conditions are not directly imposed on the density profile. For example, in self-consistent field theory (we refer to [21] for details), the profile is calculated through a propagator q, on which boundary conditions are imposed. In this case the anchoring conditions can be used on q.

To initialize the density profile for computation in our frame work, we use the setting in Fig. 1. We first choose a common period in the y- and the z- direction for phase α and β, and then fill in the bulk profiles and anchor both ends of the region. To obtain a smooth initial value, the density profile in the middle region is set as the convex combination of the bulk densities as in (3).

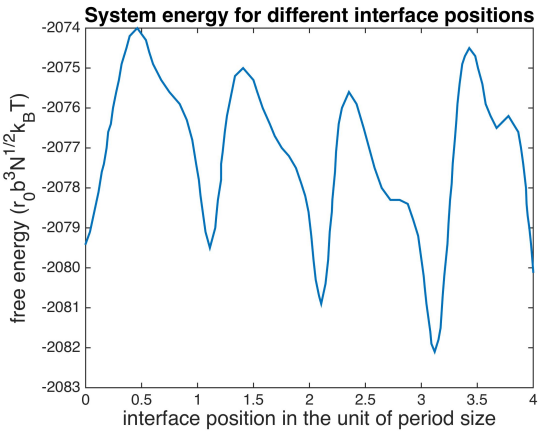

Fig. 2: Energy landscape in the movement of cylindral-gyroid interface in the Landau-Brazovskii model (8) within a single period. The parameters in (8) are chosen as $\xi^2 = 1.0$, $\tau = -0.383$, $\gamma = 0.3$. The location of interface is calculated from the distance between the points on the minimal energy path [23, 24]. The distance is measured by the unit cell of gyroid, which is rescaled to four (the upper bound of the x-axis). For the morphology at local minima, see Fig. 4. Although we choose different parameters, the morphology is identical.

2.2 Existence of local minima

Before solving the optimization problem, the well-posedness of this setting should be discussed. Specifically, we need to demonstrate the existence of local minima in our setting. It is obvious that for disorder-disorder interface, if there exists a difference in the bulk energy densities, no matter how small it is, the interface would move continuously to the one with higher energy density. In this case, the total energy can be written as

$$E = f_\alpha V_\alpha + f_\beta V_\beta + \gamma S \tag{7}$$

where f is the free energy density, V is the volume of each phase, S is the area of interface, and γ is the interfacial energy density. The isotropy of two phases along the x-direction makes γ independent of interface location. Suppose $f_\alpha < f_\beta$, then E is monotone decreasing when V_α increases, driving the interface to the phase β. For homogeneous phases, a constraint like (2) is usually easy to propose to fix the volume fraction of each phase. Nevertheless, it is difficult to extend to modulated phases.

Fortunately, we can take advantage of the anisotropy in modulated phases. The anisotropy implies that γ is no longer constant. Intuitively we write $\gamma = \gamma(x)$ as a function of interface location, and still write the total energy as (7). If $\gamma(x)$ varies more drastically than the bulk energy difference, some local minima exist, towards which we may let the interface relax. Such condition is easier to be attained when the energy difference between two phases is not large. This can be achieved when model parameters lie in a region near the binodal line. In fact, if the parameters are far away from the binodal line, usually it is difficult for the interfaces to exist for long time, for the phase with higher energy density is more probable to decompose because of fluctuations.

A typical energy landscape is like what is plotted in Fig. 2, where we compute the cylindral-gyroid interfaces in the Landau-Brazovskii model (8). It shows clearly that the energy de-

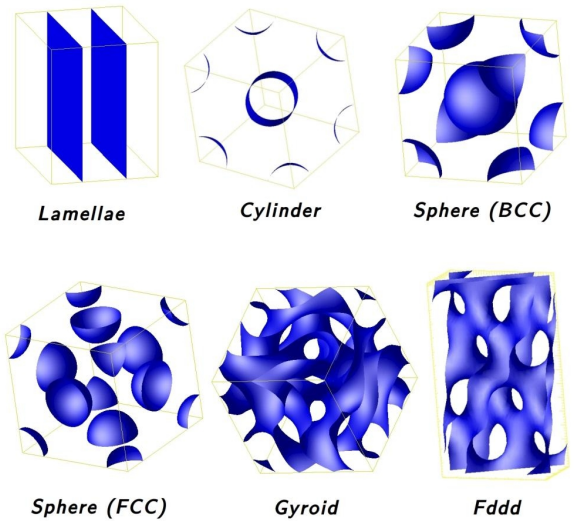

Fig. 3: Bulk phases of the Landau-Brazovskii model.

creases in a wavy manner as the interface moves. Four local minima are found within a single period along the x-direction, and they are connected with the minimum energy path computed using string method [23, 24]. The morphology of interfaces at local minima is drawn in Fig. 4 (where we draw the interfaces within two periods).

We note that only a few works study interfaces between different modulated phases with such a weak anchoring condition. The reason could be the lack of knowledge of the existence of local minima produced by modulated structures. Although in the current work it is only confirmed in one model, we believe that this phenomenon is generic, and that the clarification of the energy landscape would be helpful to the computation of interfacial structure in other systems.

3 Application to the Landau-Brazovskii model

In this section, we apply our framework for interface to the Landau-Brazovskii (LB) model. We first present the cylindral-gyroid and lamellar-gyroid interfaces in epitaxially matching cases, in which the local minima are shown clearly. Furthermore, a few novel examples of non-matching cases are given to show the effectiveness of the framework.

3.1 The free energy

The LB model is a free energy functional appropriate for weak crystallization [25, 26, 27]. This model can be viewed as a generic model for modulated phases occurring in a variety of physical and chemical systems, and its form is similar to many Landau-type free energy functionals for different kinds of materials. In addition, the LB model can describe frequently observed patterns, including lamellar(L), cylindral(C), spherical and gyroid(G) structures. Therefore our results could reveal properties of interfaces in a wide range of systems. In its

scaled form, the LB free energy density is given by

$$F[\phi] = \frac{1}{V}\int_{\Omega} \mathrm{d}\boldsymbol{r}\{\frac{\xi^2}{2}[(\nabla^2 + q_0^2)\phi]^2\} + \frac{\tau}{2}\phi^2 - \frac{\gamma}{3!}\phi^3 + \frac{1}{4!}\phi^4, \tag{8}$$

where $q_0 = 1$ is the critical wavelength, $\xi,\ \tau,\ \gamma$ are phenomenological parameters, and ϕ is conserved,

$$\int \mathrm{d}\boldsymbol{r}\phi = 0.$$

The parameters can be determined by measurable parameters in some cases. An example is the system of A-B diblock copolymer, in which these parameters are derived from χN and f, where χN is a normalized parameter characterizing the segregation of two blocks, and f is the fraction of block A. The phases in the LB model can be easily recognized by the isosurface of ϕ, drawn in Fig. 3. For the interfaces, we will also draw the isosurface to reveal their structures.

3.2 Boundary conditions

Bulk values of ϕ are needed for setting initial and boundary values of the problem. They are obtained by minimizing (8) with periodic boundary condition in all three directions. The existence of second-order derivatives in the energy functional requires ϕ and $\nabla\phi$ to be fixed at $x = \pm L$. These values can be easily computed with bulk profiles.

When computing bulk profiles, the period lengths should be optimized as well. This is because the size of the cell also affects the energy density of the system. Refined computation shows that for different phases, there is slight distinction between the optimal size of unit cell [28]. When two phases coexist, however, it is usually observed experimentally that two unit cells match each other [29, 30, 31, 32]. To capture the interfacial structure in our framework, we slightly stretch the two bulks to let them have common period lengths. Then our framework for the interface could be applied directly. Such approximation leads to a small amount of the bulk energy increase, but we will adopt it as it is consistent with experimental results. It should be pointed out that besides the period matching, different modulated structures have certain preferences in orientation when they coexist, namely the rotations $\mathcal{R}_\alpha,\ \mathcal{R}_\beta$ and the shifts $\boldsymbol{b}_\alpha,\ \boldsymbol{b}_\beta$ prefer certain values. Such epitaxial relationships are also noted in the experimental works mentioned above, and are studied in [20] extensively. We will examine such epitaxies as well as less optimal matching cases for the interfacial systems.

The profiles of L, C and G are calculated with the common period $2\sqrt{6}\pi \times 2\sqrt{6}\pi \times 2\sqrt{6}\pi$, which is almost accurate for L and C, while about 4% smaller for G. The number of meshes used in a unit cell is $32 \times 32 \times 32$. Details of discretization and optimization method are given in Appendix, in which acceleration techniques are included.

3.3 C-G and L-G interfaces

We start from the cases in which two phases are epitaxially matched: in the lattice of G, the layer of L parallels to the plane $(11\bar{2})$ and the hexagonal lattice of C lies in the plane (111). The results in Fig. 4 are calculated with $\xi^2 = 0.0389,\ \gamma = 0.0681;\ \tau = -0.0121$ for C-G interfaces and $\tau = -0.0159$ for L-G interfaces. Fig. 4 presents C-G and L-G interfaces at local energy minima. Both C-G and L-G interfaces show four local minima within one

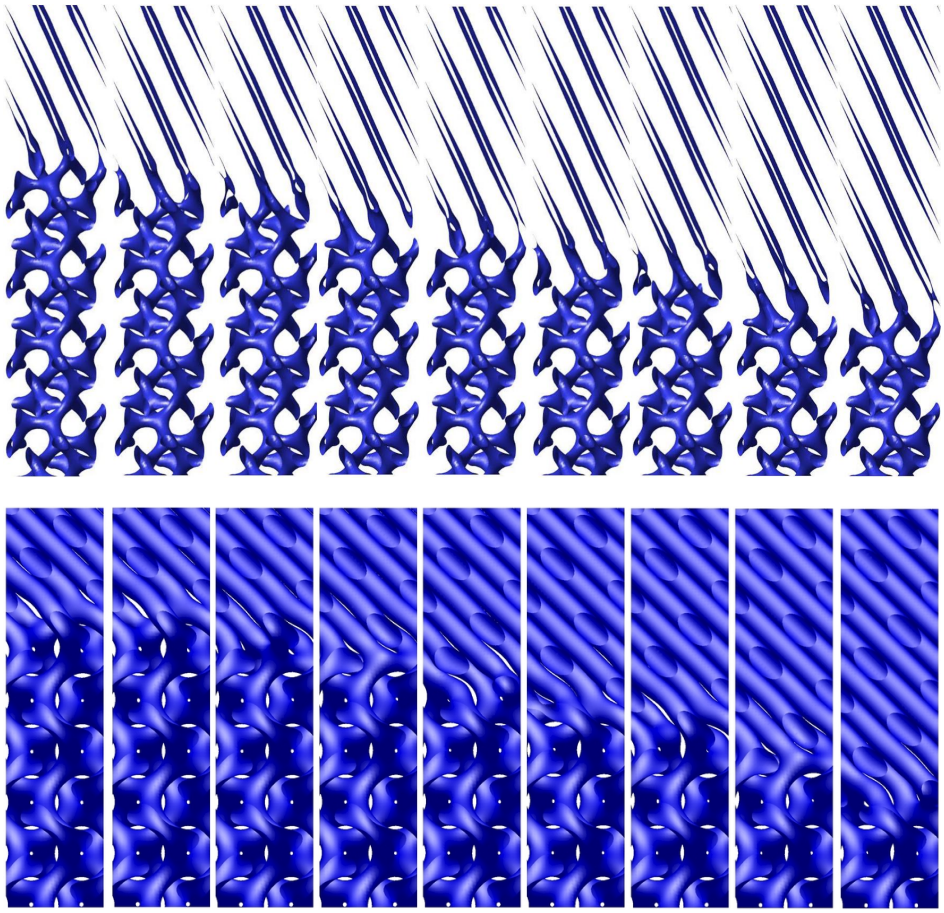

Fig. 4: L-G and C-G interfaces at local minima (within two periods): the epitaxially matching case.

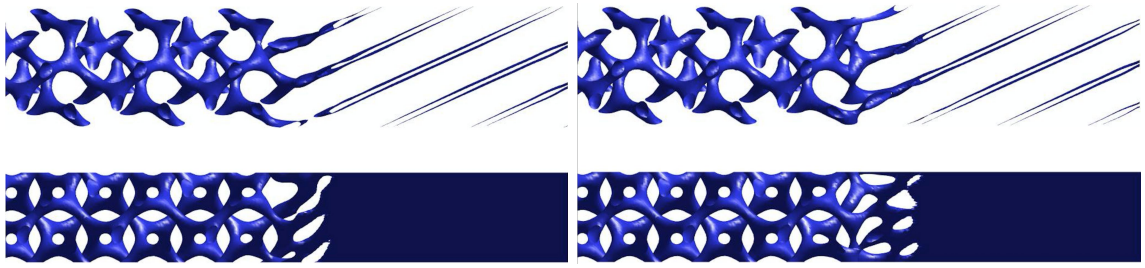

Fig. 5: The L-G interface. Left: the epitaxially matching case; Right: L is shifted a half period. Viewed along the layer of L (upper) and the unit cell of G (lower).

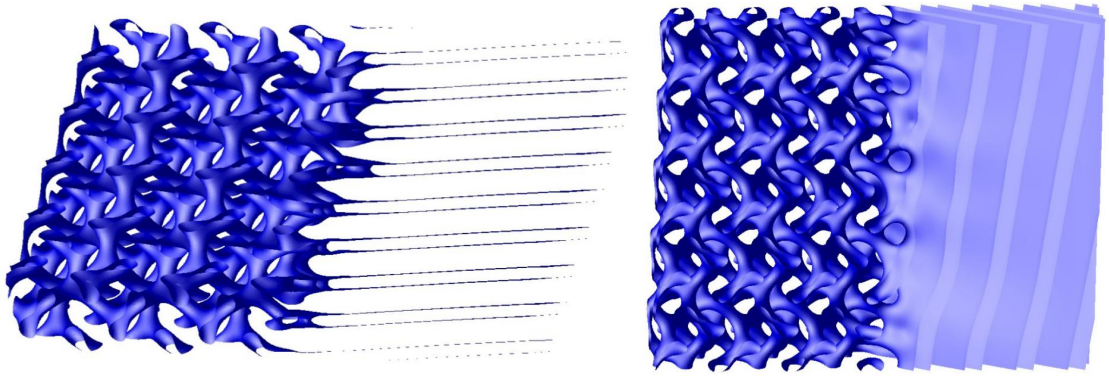

Fig. 6: L-G interfaces with L rotated counter-clockwise $\theta = \arcsin(3/5)$ (left), and $\theta + \pi/2$ (right).

period, and when moving a full period, the interfacial structures reappear. We are also able to capture how the interface moves from the ones at discrete locations.

In the following, we will present some results of the non-matching cases, in which we can observe some interesting phenomena. The results described in this paragraph are calculated with $\xi^2 = 0.0389$, $\gamma = 0.0601$, $\tau = -0.0121$. First, we examine the case where L is shifted a half period (Fig. 5 right). Comparing it with the epitaxially matching case (Fig. 5 left), we find the structure distinct from L and G in the middle. It resembles the metastable perforated layer structure, supporting the prevalent observation of perforated layer phase in the L$\leftrightarrow$G transitions (see the discussion in [33]). Next we look at the effects of relative rotation. In Fig. 6 L is rotated $\theta = \arcsin(3/5)$ and $\theta + \pi/2$ counter-clockwise respectively, G unchanged. Local distortions help to keep their connection, leading to non-planar interfaces.

The next pair of examples are based on the newly-found epitaxially relationship between C and G [32], where the lattice of C is slightly deformed from the regular hexagon and lies in the plane $(1\bar{1}0)$. The parameters are chosen as $\xi^2 = 0.0375$, $\gamma = 0.0757$, $\tau = -0.0102$. The interface is drawn in the left of Fig. 7, which is planar with smooth connection. The right of Fig. 7 shows the interface where C is rotated $\pi/2$ in the x-y plane. To connect two phases, C of the regular hexagonal type with classical epitaxy appears in between.

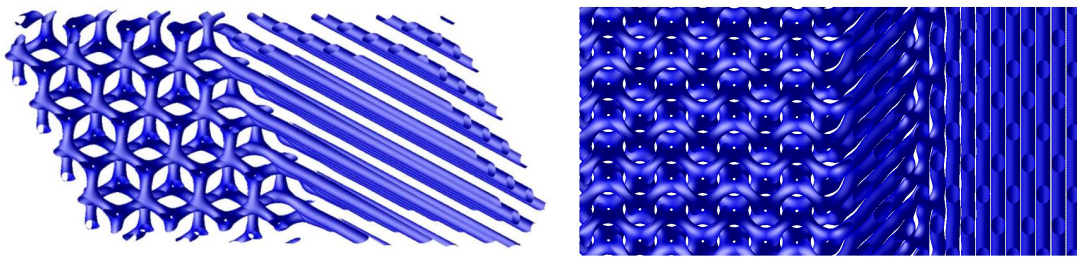

Fig. 7: Left: C-G interface with newly found epitaxy $(1\bar{1}0)$. Right: C is rotated $\pi/2$ from the new epitaxy and cylinder along $\langle 111 \rangle$ direction is found in between.

4 Summary

A general framework is proposed for the computation of interfacial structures between modulated phases. The boundary conditions and the basis functions are carefully chosen to anchor the bulk phases with given position and orientation with compatibility. Because of the anistropy in the modulated structure, no extra constraint is necessary to stabilize the interface. In this way, the optimal interfacial structure is posed as a minimization problem that enables us to reach full relaxation and utilize fast optimization methods. We apply the framework to Landau-Brazovskii model. L-G and C-G interfaces with various relative positions and orientations are investigated, where some complex structures are obtained.

So far we show the application of the framework to special cases where public period can be found in the y-z plane. The choice of basis functions (6) actually allows us to investigate quasiperiodic phases. Thus in the future we aim to apply this framework to broader cases, especially for quasiperiodic phases.

Acknowldegment Pingwen Zhang is partly supported by National Natural Science Foundation of China (Grant No. 11421101, No. 11421110001 and No. 21274005).

A Numerical details

We describe some numerical details of discretization and optimization. For the discretization of density profile, finite difference scheme is adopted in the x-direction. In the y-z plane, both finite difference scheme and Fourier expansion can be used.

In the x-direction, Laplacian is approximated by

$$\partial_x^2 \phi(x_k) \approx \delta_x^2 \phi(x_k) = \frac{\phi_{k+1} - 2\phi_k + \phi_{k-1}}{\Delta x^2}.$$

The same approximation is adopted when using finite difference scheme in the y-z plane. When using Fourier expansion in the y-z plane, we write ϕ as

$$\phi(x, y, z) = \sum_{\boldsymbol{G}} \phi_{\boldsymbol{G}}(x) \exp(i(\boldsymbol{G} \cdot \boldsymbol{r}')).$$

where $\boldsymbol{G} = m\boldsymbol{b}_1' + n\boldsymbol{b}_2'$, $\quad |m|, |n| \leq N$, $\boldsymbol{b}_i'$ are reciprocal vectors with respect to the lattice in the y-z plane, and $\boldsymbol{r}' = (y, z)$. Note that ϕ is real-valued, thus it requires $\phi_{-\boldsymbol{G}}(x) = \phi_{\boldsymbol{G}}^*(x)$.

The anchoring boundary conditions at $x = \pm L$ are implemented by adding two extra grids on each side and setting ϕ equal to bulk values. This can be equivalently viewed as approximating boundary conditions with finite difference scheme,

$$\phi(-L) = \phi_\alpha(-L), \qquad \partial_x\phi(-L) \approx \frac{\phi_0 - \phi_{-1}}{\Delta x} = \frac{\phi_\alpha(x_0) - \phi_\alpha(x_{-1})}{\Delta x} \approx \partial_x\phi_\alpha(-L).$$

The gradient vector can be calculated by

$$\nabla\tilde{F}(\phi(x)) = \xi^2[(\delta_x^2 + \delta_y^2 + \delta_z^2 + 1)^2 + \tau]\phi(x) - \frac{\gamma}{2}\phi^2(x) + \frac{1}{6}\phi^3(x)$$

for finite difference method, and by

$$\nabla\tilde{F}(\phi_{\boldsymbol{G}}(x)) = \xi^2[(\delta_x^2 - \boldsymbol{G}^2 + 1)^2 + \tau]\phi_{\boldsymbol{G}} - \frac{\gamma}{2}\sum_{\boldsymbol{G}_1+\boldsymbol{G}_2=\boldsymbol{G}} \phi_{\boldsymbol{G}_1}\phi_{\boldsymbol{G}_2} + \frac{1}{6}\sum_{\boldsymbol{G}_1+\boldsymbol{G}_2+\boldsymbol{G}_3=\boldsymbol{G}} \phi_{\boldsymbol{G}_1}\phi_{\boldsymbol{G}_2}\phi_{\boldsymbol{G}_3} \tag{9}$$

for Fourier expansion. The convolution sum can be calculated by FFT.

The conservation of ϕ is attained by a projection on the gradient vector: for finite difference scheme, we use

$$\nabla F(\phi(x)) = \nabla\tilde{F}(\phi(x)) - c;$$

and for Fourier expansion, we use

$$\nabla F(\phi_{\boldsymbol{G}}(x)) = \nabla\tilde{F}(\phi_{\boldsymbol{G}}(x)) - c\delta(\boldsymbol{G} = 0).$$

In the above, c can be determined by the following observation: if we set $\phi = \phi_\alpha$ for $x < 0$ and $\phi = \phi_\beta$ for $x > 0$, the constraint is satisfied. So we can just require

$$\int_S\int_{-L}^{L} \phi \mathrm{d}x\mathrm{d}y\mathrm{d}z = \int_S \mathrm{d}y\mathrm{d}z(\int_{-L}^{0}\phi_\alpha \mathrm{d}x + \int_0^L \phi_\beta \mathrm{d}x) \triangleq c_0.$$

For finite difference scheme, we use a gradient method

$$\phi^{n+1}(x) - \phi^n(x) = -a_n\nabla F(\phi^n(x)).$$

The coefficient a_n is altered adaptively with Barzilai-Borwein method [34, 35]. For Fourier expansion we use a semi-implicit scheme to solve the Euler-Langrange equation (9) with

$$\begin{aligned}\frac{\phi_{\boldsymbol{G}}^{n+1}(x) - \phi_{\boldsymbol{G}}^n(x)}{\Delta t} &= -\xi^2[(\delta_x^2 - \boldsymbol{G}^2 + 1)^2 + \tau]\phi_{\boldsymbol{G}}^{n+1} \\ &\quad + \frac{\gamma}{2}\sum_{\boldsymbol{G}_1+\boldsymbol{G}_2=\boldsymbol{G}} \phi_{\boldsymbol{G}_1}^n\phi_{\boldsymbol{G}_2}^n - \frac{1}{6}\sum_{\boldsymbol{G}_1+\boldsymbol{G}_2+\boldsymbol{G}_3=\boldsymbol{G}} \phi_{\boldsymbol{G}_1}^n\phi_{\boldsymbol{G}_2}^n\phi_{\boldsymbol{G}_3}^n \\ &\quad - c\delta(\boldsymbol{G} = 0).\end{aligned}$$

References

[1] J. W. Cahn and J. E. Hilliard. Free Energy of a Nonuniform System. I. Interfacial Free Energy. *J. Chem. Phys.*, 28(2):258–267, 1958.

[2] J. W. Cahn and J. E. Hilliard. Free Energy of a Nonuniform System. III. Nucleation in a Two-Component Incompressible Fluid. *J. Chem. Phys.*, 31(3):688–699, 1959.

[3] W. E. McMullen and D. W. Oxtoby. The equilibrium interfaces of simple molecules. *J. Chem. Phys.*, 88(12):7757–7765, 1988.

[4] V. Talanquer and D. W. Oxtoby. Nucleation on a solid substrate: A density-functional approach. *J. Chem. Phys.*, 104(4):1483–1492, 1996.

[5] V. Talanquer and D. W. Oxtoby. Nucleation in a slit pore. *J. Chem. Phys.*, 114(6):2793–2801, 2001.

[6] Z. Y. Chen and J. Noolandi. Numerical solution of the Onsager problem for an isotropic-nematic interface. *Phys. Rev. A*, 45(4):2389–2392, 1991.

[7] W. E. McMullen and B. G. Moore. Theoretical Studies of the Isotropic-Nematic Interface. *Mol. Cryst. Liq. Cryst.*, 198(1):107–117, 1991.

[8] T. M. Rogers and R. C. Desai. Numerical study of late-stage coarsening for off-critical quenches in the Cahn-Hilliard equation of phase separation. *Phys. Rev. B*, 39(16):11956–11964, 1989.

[9] C. Liu and J. Shen. A phase field model for the mixture of two incompressible fluids and its approximation by a Fourier-spectral method. *Physica D*, 179(3-4):211–228, 2003.

[10] R. R. Netz, D. Andelman, and M. Schick. Interfaces of Modulated Phases. *Phys. Rev. Lett.*, 79(6):1058–1061, 1997.

[11] M. W. Masten. Kink grain boundaries in a block copolymer lamellar phase. *J. Chem. Phys.*, 107(19):8110–8119, 1997.

[12] Y. Tsori, D. Andelman, and M. Schick. Defects in lamellar diblock copolymers: Chevron- and ω-shaped tilt boundaries. *Phys. Rev. E*, 61(3):2848–2858, 2000.

[13] D. Duque, K. Katsov, and M. Schick. Theory of T junctions and symmetric tilt grain boundaries in pure and mixed polymer systems. *J. Chem. Phys.*, 117(22):10315–10320, 2002.

[14] A. Jaatinen, C. V. Achim, K. R. Elder, and T. Ala-Nissila. Thermodynamics of bcc metals in phase-field-crystal models. *Phys. Rev. E*, 80:031602, 2009.

[15] M. Belushkin and G. Gompper. Twist grain boundaries in cubic surfactant phases. *J. Chem. Phys.*, 130:134712, 2009.

[16] K. R. Elder and M. Grant. Modeling elastic and plastic deformations in nonequilibrium processing using phase field crystals. *Phys. Rev. E*, 70:051605, 2004.

[17] A. V. Kyrylyuk and J. G. E. M. Fraaije. Three-Dimensional Structure and Motion of Twist Grain Boundaries in Block Copolymer Melts. *Macromolecules*, 38:8546–8553, 2005.

[18] A. D. Pezzutti, D. A. Vega, and M. A. Villar. Dynamics of dislocations in a two-dimensional block copolymer system with hexagonal symmetry. *Phil. Trans. R. Soc. A*, 369:335–350, 2011.

[19] K. Yamada and T. Ohta. Interface between Lamellar and Gyroid Structure in Diblock Copolymer Melts. *Journal of the Physical Society of Japan*, 76(8):084801, 2007.

[20] C. Wang, K. Jiang, P. Zhang, and A. C. Shi. Origin of epitaxies between ordered phases of block copolymers. *Soft Matter*, 7:10552–10555, 2011.

[21] G. H. Fredrickson. *The equilibrium theory of inhomogeneous polymers*. Clarendon Press, Oxford, 2006.

[22] K. L. Merkle. High-Resolution Electron Microscopy of Grain Boundaries. *Interface Sceince*, 2:311–345, 1995.

[23] W. E, W. Ren, and E. V. Eijnden. String method for the study of rare events. *Phys. Rev. B*, 66:052301, 2002.

[24] W. E, W. Ren, and E. V. Eijnden. Simplified and improved string method for computing the minimum energy paths in barrier-crossing events. *J. Chem. Phys.*, 126:164103, 2007.

[25] S. A. Brazovskii. Phase transition of an isotropic system to a nonuniform state. *Sov. Phys.-JETP*, 41(1):85–89, 1975.

[26] G. H. Fredrickson and E. Helfand. Fluctuation effects in the theory of microphase separation in block copolymers. *J. Chem. Phys.*, 87(1):697–705, 1987.

[27] E. I. Kats, V. V. Lebedev, and A. R. Muratov. Weak crystallization theory. *Physics reports*, 228(1):1–91, 1993.

[28] P. Zhang and X. Zhang. An efficient numerical method of Landau-Brazovskii model. *J. Comput. Phys.*, 227:5859–5870, 2008.

[29] M. F. Schulz, F. S. Bates, K. Almdal, and K. Mortensen. Epitaxial Relationship for Hexagonal-to-Cubic Phase Transition in a Block Copolymer Mixture. *Phys. Rev. Lett.*, 73(1):86–89, 1994.

[30] D. A. Hajduk, S. M. Gruner, P. Rangarajan, R. A. Register, L. J. Fetters, C. Honeker, R. J. Albalak, and E. L. Thomas. Observation of a Reversible Thermotropic Order-Order Transition in a Diblock Copolymer. *Macromolecules*, 27:490–501, 1994.

[31] J. Bang and T. P. Lodge. Mechanisms and Epitaxial Relationships between Close-Packed and BCC Lattices in Block Copolymer Solutions. *J. Phys. Chem. B*, 107(44):12071–12081, 2003.

[32] H. W. Park, J. Jung, T. Chang, K. Matsunaga, and H. Jinnai. New Epitaxial Phase Transition between DG and HEX in PS-*b*-PI. *J. Am. Chem. Soc.*, 131:46–47, 2009.

[33] X. Cheng, L. Lin, W. E, P. Zhang, and A. C. Shi. Nucleation of Ordered Phases in Block Copolymers. *Phys. Rev. Lett.*, 104:148301, 2010.

[34] J. Barzilai and J. M. Borwein. Two-point step size gradient methods. *IMA J. Numer. Anal.*, 8:141–148, 1988.

[35] B. Zhou, L. Gao, and Y. H. Dai. Gradient Methods with Adaptive Step-Sizes. *Computational Optimization and Applications*, 35:69–86, 2006.